JOURNAL OF THEORETICAL
AND APPLIED MECHANICS
4, **39**, 2001

COHERENT STRUCTURES AND TRANSPORT OF TEMPERATURE VARIANCE AND OSCILLATORY HEAT FLUXES IN A STIMULATED ROUND JET

Stanisław Drobniak
Roman Klajny
Piotr Pełka

Institute of Thermal Machinery, Technical University of Częstochowa
e-mail: imc@imc.pcz.czest.pl

The paper deals with heat transfer processes taking place in the near flow region of axisymmetric free jet in the presence of coherent motion stimulated by acoustic wave. The parameters selected for qualitative and quantitative analysis were the temperature variance and coherent as well as oscillatory heat fluxes. Temperature variance was treated as a measure of intensity of heat transport while heat fluxes described spatial characteristics of the heat transfer processes. Analysis of transport equations of the above quantities should explain the physics of heat transfer realised in the presence of coherent structures.

Key words: turbulent jet, coherent structures, temperature variance

Notation

a	–	thermal diffusivity
c_p	–	specific heat capacity of air at constant pressure
D	–	exit nozzle diameter
f	–	excitation frequency
P, p	–	pressure
Re	–	Reynolds number
St	–	Strouhal number
T	–	period of oscillatory motion
t	–	time
U, u	–	velocity
x, r, φ	–	cylindrical coordinate system

Θ, ϑ	–	temperature
λ_s	–	wavelength of the coherent structure
ρ	–	density
ν	–	kinematic viscosity

and $(\bar{\cdot})$ – time-mean average; $(\tilde{\cdot})$ – oscillatory component; $(\cdot')$ – random component; $\langle\cdot\rangle$ – phase averaging operator, and subscripts: a – ambient conditions; o – nozzle outlet; r – radial direction; x – axial direction; φ – circumferential direction.

1. Introduction and experimental conditions

The research performed at the Institute of Thermal Machinery in the field of transport properties of internal (El Sayed, 1995) and kinetic energy revealed the important role of coherent motion. The object of the research was the non-isothermal round jet issuing from the contoured nozzle of $D = 0.04\,\mathrm{m}$ at the constant exit velocity corresponding to the Reynolds number

$$\mathrm{Re} = 40000$$

The overheat of the flowing medium (i.e. the difference between the ambient $\overline{\Theta_a}$ and exit air temperature $\overline{\Theta_o}$) was kept at the constant level of

$$\Delta\overline{\Theta} = \overline{\Theta_a} - \overline{\Theta_o} = 40^\circ\mathrm{C}$$

i.e. the experiment was confined to "weakly-non-isothermal" range because of the requirements resulting from the hot-wire technique.

The free, round jet reveals a multi-modality of the coherent motion (Drobniak, 1986; Drobniak and Elsner, 1986; Wygnański and Peterson, 1987), and that is why the flow had to be externally stimulated by the harmonic acoustic wave of the frequency f given by the Strouhal number

$$\mathrm{St} = \frac{fD}{U_o} = 0.42$$

The above value corresponds to the so-called "alternate-mode", which on the one hand is characterised by the largest amplitudes attained and, on the other hand, by the absence of pairing, which could disturb the mechanism analysed. The acoustic jet stabilisation cancelled the random dispersion of size and shedding frequency of coherent vortices and furthermore, enabled us to use the acoustic pressure as a reference signal in the phase-averaging procedure.

In the course of experiment, the three components of instantaneous velocity together with the instantaneous temperature have been recorded with the use of a combined four-wire sensor, described in detail in (El Sayed et al., 1998). The discussion of data processing algorithms was given in (Drobniak et al., 1998). The three test cross-sections selected for the analyses were located in the cross-sections characterised by the growth $(x/D = 1.5)$, the maximum spatial coherence $(x/D = 2.5)$ and decay $(x/D = 4)$ of the column mode vortices. The above main cross-sections were accompanied by auxiliary measuring planes, which were needed to determine the gradients of particular quantities in the transport equation analysed. The $\varDelta x$ distance between main and auxiliary planes was selected as $\varDelta x/\lambda_s = 0.08$ (i.e. $\varDelta x/D = 0.125$), because the results of preliminary measurements (Elsner et al., 1992; Elsner and Drobniak, 1994) as well as the literature data (Favre-Marinet, 1986, 1989) have shown that this value was on the one hand sufficiently small in comparison with the wavelength λ_s of the structures and, on the other hand, it was large enough to obtain accurate estimation of the particular gradients in the equations considered.

2. Basic assumptions used in formulation of transport equations

The starting point for formulation of transport equations for temperature variances and heat fluxes was the triple decomposition concept introduced in (Reynolds and Hussain) which may be written for the arbitrary flow field quantity as follows

$$F(x_i,t) = \overline{F}(x_i) + \widetilde{f}(x_i,t) + f'(x_i,t) \tag{2.1}$$

where $\overline{F}(x_i)$ – time-mean quantity, $\widetilde{f}(x_i,t)$ – periodic component, $f'(x_i,t)$ – random component. Following the above concept, the velocity U_i, pressure P and temperature $\varTheta$ could be the decomposed as follows

$$U_i = \overline{U_i} + \widetilde{u}_i + u_i \qquad \varTheta = \overline{\varTheta} + \widetilde{\vartheta} + \vartheta \qquad P = \overline{P} + \widetilde{p} + p' \tag{2.2}$$

where $i = x, r, \varphi$ stand for the axisymmetric coordinates applied. If one assumes relatively small velocity range, as well as a moderate overheat of the jet, then it will be possible to consider the flow as incompressible with constant physical properties, such as viscosity ν, thermal diffusivity α, etc. In addition to time-averaging, the phase-averaging operator was introduced according to the formula

$$
\langle F\rangle = \lim_{N\to\infty}\Big[\frac{1}{N}\sum_{p=1}^{n} F(t+p\widetilde{T})\Big] = \overline{F} + \widetilde{f} \tag{2.3}
$$

where $\widetilde{T}$ was the period of oscillatory motion and N denoted the number of averaged periods. The phase reference was the acoustic pressure signal used for flow stimulation. The details of derivation of the transport equations analysed were given in (Pełka, 1999).

3. Budget of oscillatory component of temperature variance

The transport equations for oscillatory component of temperature variance in axisymmetric coordinates may be written as follows

$$
\begin{aligned}
&\underbrace{\overline{U_x}\frac{\partial}{\partial x}\Big(\frac{\overline{\widetilde{\vartheta}^2}}{2}\Big) + \overline{U_r}\frac{\partial}{\partial r}\Big(\frac{\overline{\widetilde{\vartheta}^2}}{2}\Big)}_{(1)} - \underbrace{\frac{1}{\rho c_p}\Big\{\overline{\overline{U_x}\widetilde{\vartheta}\frac{\partial\widetilde{p}}{\partial x}} + \overline{\overline{U_r}\widetilde{\vartheta}\frac{\partial\widetilde{p}}{\partial r}} + \overline{\widetilde{u}_x\widetilde{\vartheta}\frac{\partial p}{\partial x}} + \overline{\widetilde{u}_r\widetilde{\vartheta}\frac{\partial p}{\partial r}} +}_{(2)}\\
&\underbrace{+\overline{\widetilde{\vartheta}\frac{\partial}{\partial x}\Big(\widetilde{u}_x\widetilde{p}+\langle u_x'p'\rangle\Big)} + \overline{\widetilde{\vartheta}\frac{1}{r}\frac{\partial}{\partial r}\Big[r\Big(\widetilde{u}_r\widetilde{p}+\langle u_r'p'\rangle\Big)\Big]}\Big\}}_{(2)} -\\
&-\underbrace{\Big(-\overline{\widetilde{u}_x\widetilde{\vartheta}}\Big)\frac{\partial\overline{\Theta}}{\partial x} + \Big(-\overline{\widetilde{u}_r\widetilde{\vartheta}}\Big)\frac{\partial\overline{\Theta}}{\partial r}}_{(3)} + \underbrace{\overline{\widetilde{u}_x\frac{\partial}{\partial x}\Big(\frac{\widetilde{\vartheta}^2}{2}\Big)} + \overline{\widetilde{u}_r\frac{\partial}{\partial r}\Big(\frac{\widetilde{\vartheta}^2}{2}\Big)}}_{(4)} +\\
&+\underbrace{\frac{\partial}{\partial x}\Big(\overline{\widetilde{\vartheta}\langle u_x'\vartheta'\rangle}\Big) + \frac{1}{r}\frac{\partial}{\partial r}\Big(r\overline{\widetilde{\vartheta}\langle u_r'\vartheta'\rangle}\Big)}_{(5)} + \underbrace{\overline{\Big(-\langle u_x'\vartheta'\rangle\frac{\partial\widetilde{\vartheta}}{\partial x}\Big)} + \overline{\Big(-\langle u_r'\vartheta'\rangle\frac{\partial\widetilde{\vartheta}}{\partial r}\Big)}}_{(6)} -\\
&-\underbrace{a\Big[\frac{\partial^2}{\partial x^2}\Big(\frac{\overline{\widetilde{\vartheta}^2}}{2}\Big) + \frac{\partial^2}{\partial r^2}\Big(\frac{\overline{\widetilde{\vartheta}^2}}{2}\Big) + \frac{1}{r}\frac{\partial}{\partial r}\Big(\frac{\overline{\widetilde{\vartheta}^2}}{2}\Big)\Big]}_{(7)} + \underbrace{a\Big[\overline{\Big(\frac{\partial\widetilde{\vartheta}}{\partial x}\Big)^2} + \overline{\Big(\frac{\partial\widetilde{\vartheta}}{\partial r}\Big)^2}\Big]}_{(8)} = 0
\end{aligned} \tag{3.1}
$$

where terms containing $\partial/\partial\varphi$ derivatives were omitted, and symbols $(\bar{\cdot})$ and $\langle\cdot\rangle$ denoted quantities resulting from time and phase-averaging, respectively. The particular terms of these equations may be interpreted as:

(1) – Advection of Oscillatory component of Temperature Variance (AOTV)
(2) – Redistribution of Oscillatory component of temperature variance resulting from the interaction of temperature oscillations, velocity U and pressure P fields (ROUP)
(3) – Production of oscillatory component of temperature variance performed by Oscillatory Heat Fluxes (POHF)
(4) – Diffusion of Oscillatory component of Temperature Variance (DOTV)
(5) – Redistribution of oscillatory component of temperature variance performed by Modulated Heat Fluxes (RMHF)
(6) – Production of oscillatory component of temperature variance performed by Modulated Heat Fluxes (PMHF)
(7) – Redistribution of oscillatory component of temperature variance performed by Molecular Heat Transport (RMHT)
(8) – Dissipation of Oscillatory component of Temperature Variance (DsOTV).

The instantaneous temperature and velocity time-series recorded during the measurements after proper processing (El Sayed et al., 1998) allowed to calculate the values of the first four terms of Eq. (3.1), except the term (2)-(ROUP) which was treated as a closing quantity.

The above transport equation reveals that the transport of oscillatory temperature variance is realised by the following processes:

- Advection which describes the transport oscillatory variance by the mean motion (term 1).

- Redistribution of oscillatory temperature variance within the same form of fluid motion (terms 2, 4, 5, 7).

- Exchange of oscillatory temperature variance between the mean and oscillatory motion (term 3, 6),

- Dissipation which describes the viscous damping of the oscillatory variance by periodic motion (term 8).

All the terms of Eq. (3.1) were normalised by $\overline{U_0}(\varDelta\overline{\Theta})^2/D$, where $\overline{U_0}$ was the mean velocity at the jet exit.

Results of calculations have shown that the amplitudes of dissipation (term 8) and redistribution due to molecular motion (term 7) were by three orders of magnitude smaller than the remaining terms and that is why both

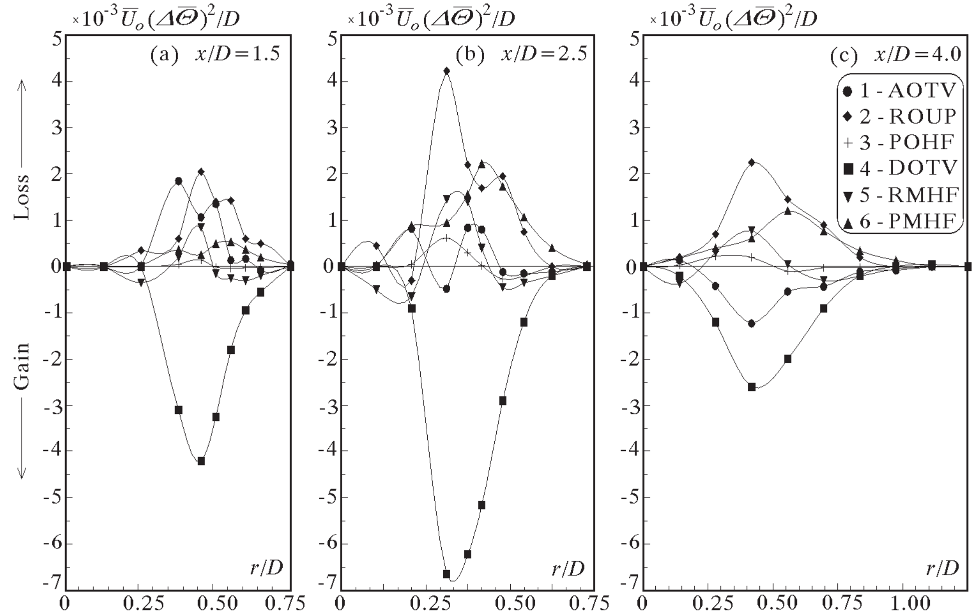

Fig. 1. Budget of oscillatory component of temperature variance at the cross-sections: (a) $x/D = 1.5$, (b) $x/D = 2.5$, (c) $x/D = 4.0$

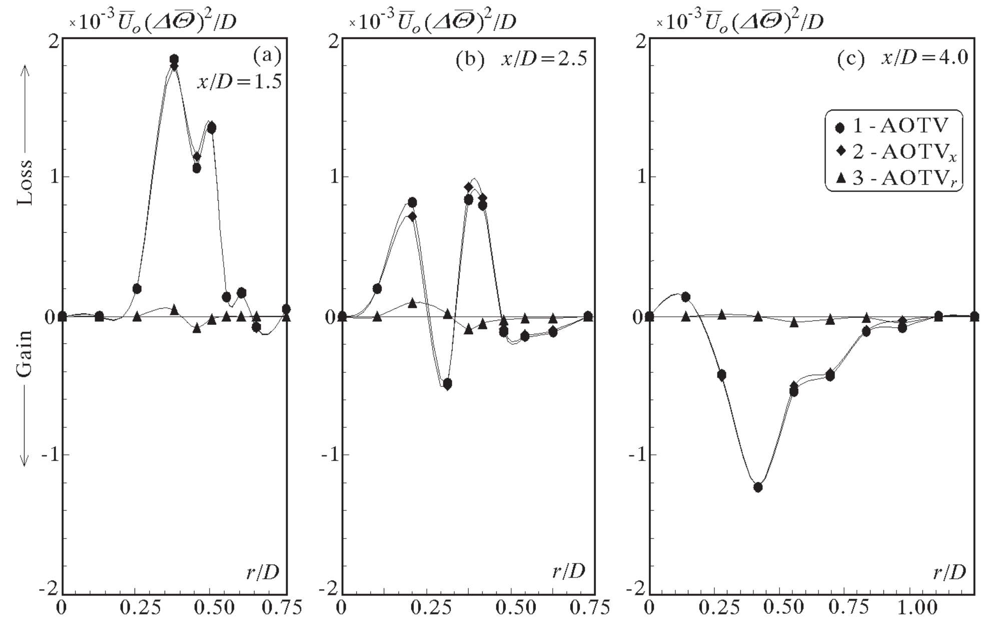

Fig. 2. Radial distributions of axial, radial and total advection of oscillatory component of temperature variance at the cross-sections: (a) $x/D = 1.5$, (b) $x/D = 2.5$, (c) $x/D = 4.0$

these terms were omitted in further analyses. The computed budget of oscillatory temperature variance was presented in Fig. 1 for the three cross-sections analysed. The data presented in this figure reveal that advection, diffusion and production are the dominating terms in the budget and that is why they were the subject of a more detailed analysis.

The advection term in axisymmetric flow $(\partial/\partial\varphi = 0)$ may be decomposed as follows

$$\mathrm{AOTV} = \underbrace{\overline{U_x}\frac{\partial}{\partial x}\Big(\frac{\overline{\widetilde{\vartheta}^2}}{2}\Big)}_{(\mathrm{AOTV}_x)} + \underbrace{\overline{U_r}\frac{\partial}{\partial r}\Big(\frac{\overline{\widetilde{\vartheta}^2}}{2}\Big)}_{(\mathrm{AOTV}_r)}$$

where (AOTV_x) denotes the axial component while (AOTV_r) is the radial component of the advection term. As it may be seen in Fig. 2, the axial component (AOTV_x) dominates practically the advection what means that the oscillatory variance is convected by the mean motion while the contribution of radial component (AOTV_r) is negligible in all the cross-sections analysed. The diffusion term contains also the axial and radial subterms denoted as follows

$$\mathrm{DOTV} = \underbrace{\overline{\widetilde{u}_x\frac{\partial}{\partial x}\Big(\frac{\widetilde{\vartheta}^2}{2}\Big)}}_{(\mathrm{DOTV}_x)} + \underbrace{\overline{\widetilde{u}_r\frac{\partial}{\partial r}\Big(\frac{\widetilde{\vartheta}^2}{2}\Big)}}_{(\mathrm{DOTV}_r)}$$

which were presented in Fig. 3. As it can be seen, both these subterms are diffused with almost equal intensity in axial and radial directions. The maximum amplitude of diffusion appears at the cross-section $x/D = 2.5$ where the maximum coherence of organised vortices is observed (Drobniak et al., 1997). The loss of temperature variance in the inner region of the jet and its gain in the outer area of the jet (see Fig. 3) results from the mixing processes realised by the fronts and backs of coherent vortices, as it has been described in (Drobniak et al., 1998).

Production of oscillatory temperature variance realised by oscillatory heat fluxes (term 4) was also decomposed into the axial and radial components denoted as

$$\mathrm{POHF} = \underbrace{\Big(-\overline{\widetilde{u}_x\widetilde{\vartheta}}\Big)\frac{\partial\overline{\Theta}}{\partial x}\Big)}_{(\mathrm{POHF}_x)} + \underbrace{\Big(-\overline{\widetilde{u}_r\widetilde{\vartheta}}\Big)\frac{\partial\overline{\Theta}}{\partial r}\Big)}_{(\mathrm{POHF}_r)}$$

and presented in Fig. 4. One may note that this type of production is dominated by radial component while the production performed by axial heat flux is close to zero in all cross-sections. Negative values of the production term (POHF_r) mark the gain of oscillatory temperature variance with the maximum values in the middle of the shear layer $r/D = 0.5$. It should be noted

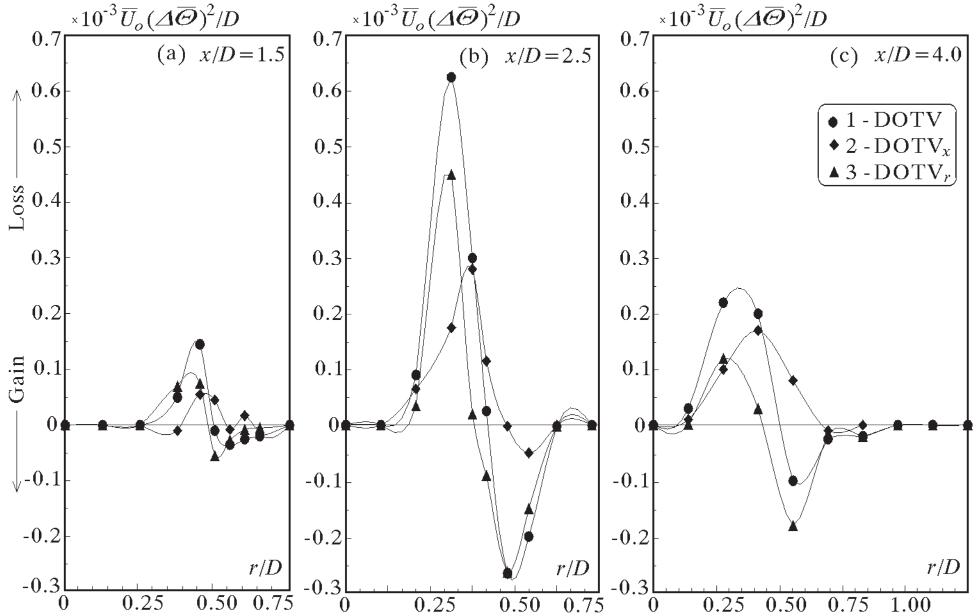

Fig. 3. Radial distributions of axial, radial and total diffusion of oscillatory component of temperature variance at the cross-sections: (a) $x/D = 1.5$, (b) $x/D = 2.5$, (c) $x/D = 4.0$

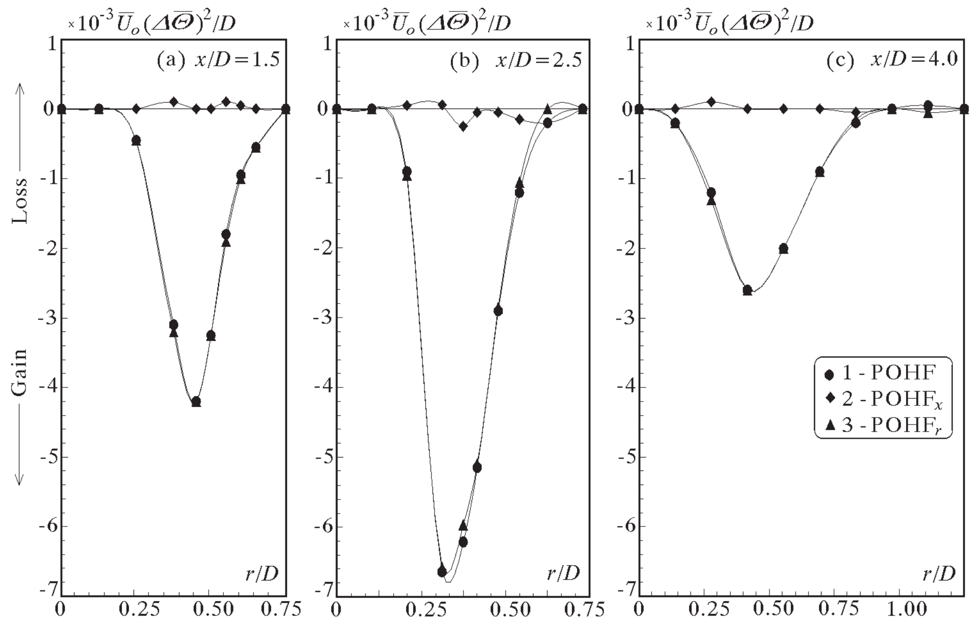

Fig. 4. Radial distributions of axial radial and total production of oscillatory component of temperature variance performed by oscillatory heat fluxes, at the cross-sections: (a) $x/D = 1.5$, (b) $x/D = 2.5$, (c) $x/D = 4.0$

that this radial location corresponds to the trajectory of vortex centres in the analysed region (Drobniak et al., 1997).

The production term due to modulated heat fluxes could be decomposed as follows

$$\mathrm{PMHF} = \underbrace{\overline{\Big(-\langle u_x'\vartheta'\rangle\frac{\partial\widetilde{\vartheta}}{\partial x}\Big)}}_{(\mathrm{PMHF}_x)} + \underbrace{\overline{\Big(-\langle u_x'\vartheta'\rangle\frac{\partial\widetilde{\vartheta}}{\partial r}\Big)}}_{(\mathrm{PMHF}_r)}$$

and their distributions are presented in Fig. 5. It may be seen from this figure that this type of production is equally intense in axial and radial directions, with the radial component slightly prevailing in the vicinity of $r/D = 0.5$ area what corresponds to the trajectory of centres of coherent vortices. All the terms presented in Fig. 5 are positive what corresponds to the loss in the budget of oscillatory temperature variance and one may find therefore that this term is responsible for conversion of the oscillatory temperature variance from periodic to random motion.

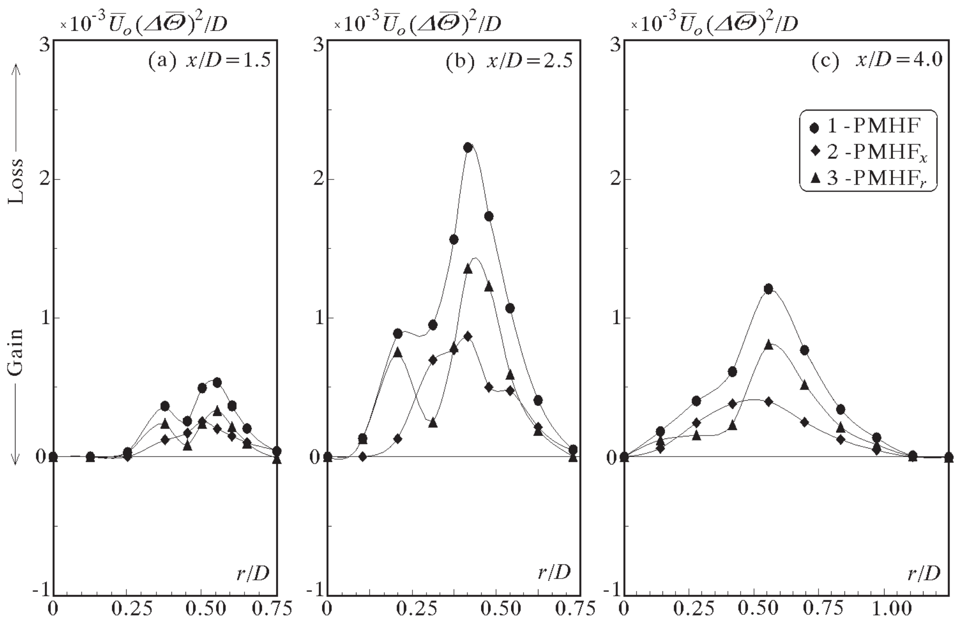

Fig. 5. Radial distributions of axial radial and total production of oscillatory component of temperature variance performed by modulated heat fluxes, at the cross-sections: (a) $x/D = 1.5$, (b) $x/D = 2.5$, (c) $x/D = 4.0$

4. Budget of random component of temperature variance

Transport equation of random component of temperature variance in axi-symmetric coordinates may be written as follows

$$\begin{aligned}
&\underbrace{\overline{U_x}\frac{\partial}{\partial x}\Big(\frac{\overline{\vartheta'^2}}{2}\Big)+\overline{U_r}\frac{\partial}{\partial r}\Big(\frac{\overline{\vartheta'^2}}{2}\Big)}_{(1)}+\frac{1}{\rho c_p}\underbrace{\Big\{\overline{\overline{U_x}\vartheta'\frac{\partial p'}{\partial x}}+\overline{\overline{U_r}\vartheta'\frac{\partial p'}{\partial r}}+\overline{\widetilde{u}_x\Big\langle\vartheta'\frac{\partial p'}{\partial x}\Big\rangle}+}_{(2)}\\
&\underbrace{+\overline{\widetilde{u}_r\Big\langle\vartheta'\frac{\partial p'}{\partial r}\Big\rangle}+\overline{u'_x\vartheta'}\frac{\partial\overline{P}}{\partial x}+\overline{u'_r\vartheta'}\frac{\partial\overline{P}}{\partial r}+\overline{\langle u'_x\vartheta'\rangle\frac{\partial\widetilde{p}}{\partial x}}+\overline{\langle u'_r\vartheta'\rangle\frac{\partial\widetilde{p}}{\partial r}}+\overline{\vartheta'\frac{\partial}{\partial x}(u'_xp')}+}_{(2)}\\
&\underbrace{+\overline{\vartheta'\frac{1}{r}\frac{\partial}{\partial r}[r(u'_rp')]}\Big\}}_{(2)}+\underbrace{\overline{u'_x\frac{\partial}{\partial x}\Big(\frac{\vartheta'^2}{2}\Big)}+\overline{u'_r\frac{\partial}{\partial r}\Big(\frac{\vartheta'^2}{2}\Big)}}_{(3)}+\\
&+\underbrace{\overline{\widetilde{u}_x\frac{\partial}{\partial x}\Big\langle\frac{\vartheta'^2}{2}\Big\rangle}+\overline{\widetilde{u}_r\frac{\partial}{\partial r}\Big\langle\frac{\vartheta'^2}{2}\Big\rangle}}_{(4)}-\underbrace{\Big(\overline{-u'_x\vartheta'}\Big)\frac{\partial\overline{\Theta}}{\partial x}-\Big(\overline{-u'_r\vartheta'}\Big)\frac{\partial\overline{\Theta}}{\partial r}}_{(5)}-\\
&-\underbrace{\overline{(-\langle u'_x\vartheta'\rangle)\frac{\partial\widetilde{\vartheta}}{\partial x}}-\overline{(-\langle u'_r\vartheta'\rangle)\frac{\partial\widetilde{\vartheta}}{\partial r}}}_{(6)}-\underbrace{a\Big[\frac{\partial^2}{\partial x^2}\Big(\frac{\overline{\vartheta'^2}}{2}\Big)+\frac{\partial^2}{\partial r^2}\Big(\frac{\overline{\vartheta'^2}}{2}\Big)+\frac{1}{r}\frac{\partial}{\partial r}\Big(\frac{\overline{\vartheta'^2}}{2}\Big)\Big]}_{(7)}+\\
&+\underbrace{a\Big[\overline{\Big(\frac{\partial\vartheta'}{\partial x}\Big)^2}+\overline{\Big(\frac{\partial\vartheta'}{\partial r}\Big)^2}}_{(8)}=0
\end{aligned}\tag{4.1}$$

Particular terms of the above equation have been interpreted as:

(1) – Advection of Random component of Temperature Variance (ARTV)

(2) – Redistribution of Random component of temperature variance resulting from the inter- action between oscillatory temperature and velocity U and pressure P fields (RRUP)

(3) – Diffusion of random component of Temperature Variance performed by Turbulent motion (DTVT)

(4) – Diffusion of random component of Temperature Variance performed by Oscillatory motion (DTVO)

(5) – Production of Random component of temperature variance performed by turbulent Heat Fluxes (PRHF)

(6) – Production of random component of temperature variance performed by Modulated Heat Fluxes (PMHF)
(7) – Redistribution of Random component of temperature variance performed by Molecular Heat transport (RRMH)
(8) – Dissipation of Random component of Temperature Variance (DsRTV).

Distribution of particular terms of Eq. (4.1) has been presented in Fig. 6. Terms 2 and 8 could not be determined during the experiment and that is why they were treated as a joint closing quantity. Term 7 presenting the redistribution of random temperature variance performed by molecular heat transport (RRMH) was considerably smaller than the remaining terms and was not shown in Fig. 6. The data presented in Fig. 6 reveal that convection, diffusion and production of random temperature variance performed by random motion dominate the budget. Convection is dominated by the subterm responsible for the transport in x-direction in the way analogous to the one shown in Fig. 2 and because of the limited space, it was not shown here.

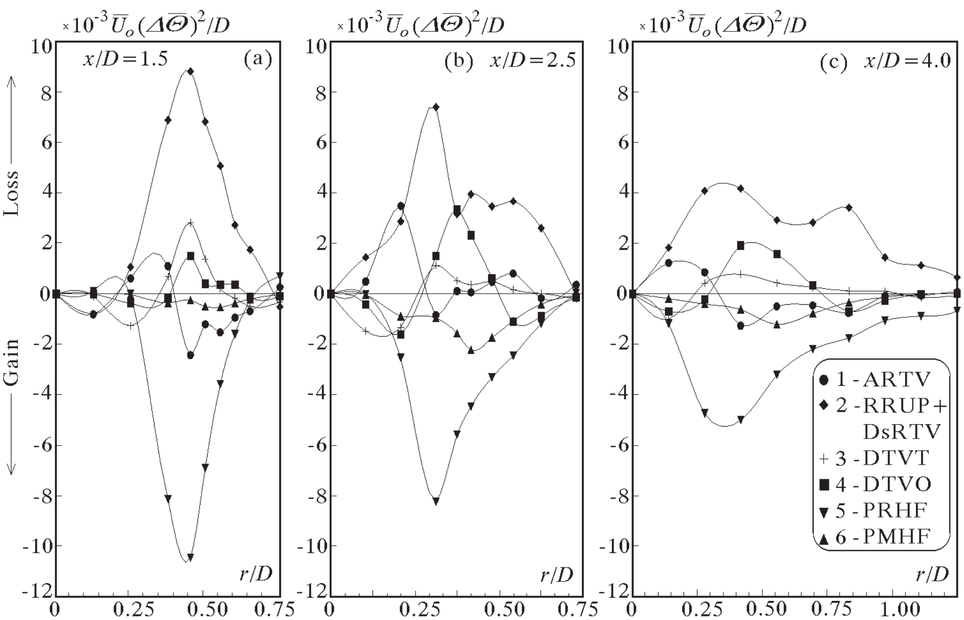

Fig. 6. Budget of random component of temperature variance at the cross-sections: (a) $x/D = 1.5$, (b) $x/D = 2.5$, (c) $x/D = 0.4$

Analysis of the diffusion term reveals that it may be divided as follows

$$\mathrm{DTVT} = \underbrace{\overline{u'_x \frac{\partial}{\partial x}\Big(\frac{\vartheta'^2}{2}\Big)}}_{(\mathrm{DTVT}_x)} + \underbrace{\overline{u'_r \frac{\partial}{\partial r}\Big(\frac{\vartheta'^2}{2}\Big)}}_{(\mathrm{DTVT}_r)}$$

and the particular subterms were presented in Fig. 7. As may be concluded from Fig. 7, diffusion of the random component of temperature variance is dominated by the radial subterm (DTVT_r) which is practically equal to total diffusion. It means therefore that the diffusion performed by random motion (DTVT) reveals a character typical for a gradient process.

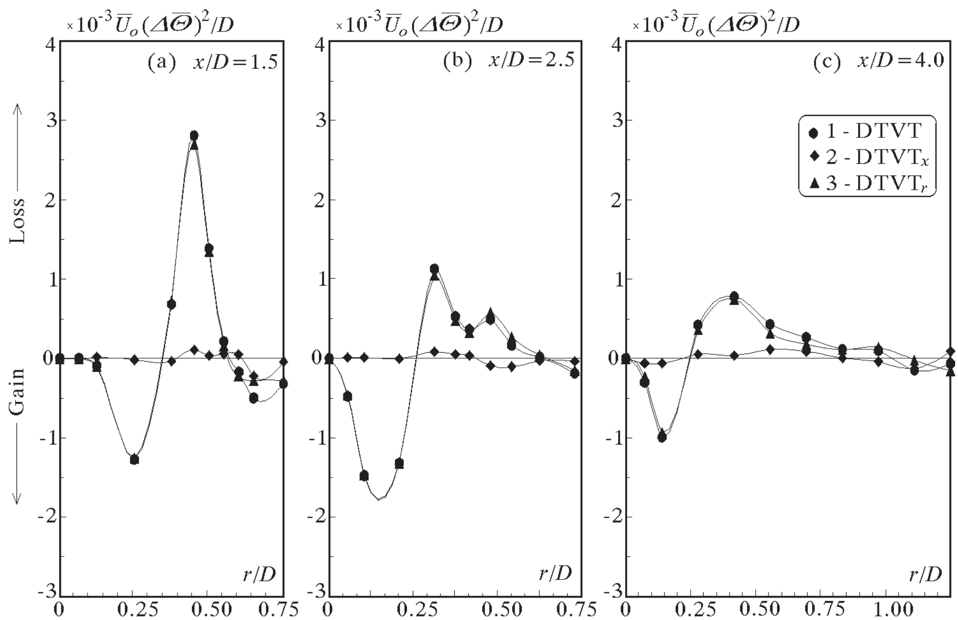

Fig. 7. Radial distributions of axial, radial and total diffusion of random component of temperature variance performed by turbulent motion at the cross-sections: (a) $x/D = 1.5$, (b) $x/D = 2.5$, (c) $x/D = 4.0$

Diffusion performed by oscillatory motion was also subdivided into two subterms, i.e.

$$\mathrm{DTVO} = \underbrace{\overline{\widetilde{u}_x \frac{\partial}{\partial x}\Big\langle\frac{\vartheta'^2}{2}\Big\rangle}}_{(\mathrm{DTVO}_x)} + \underbrace{\overline{\widetilde{u}_r \frac{\partial}{\partial r}\Big\langle\frac{\vartheta'^2}{2}\Big\rangle}}_{(\mathrm{DTVO}_r)}$$

and distribution of particular subterms as well as of total (DTVO) diffusion was shown in Fig. 8. Contrary to the case discussed in the previous section, the diffusion process performed by oscillatory motion is realised by radial and axial subterms as it is shown in Fig. 8. Total diffusion reveals a certain gain in the inner and outer jet areas while in the central region $r/D \approx 0.5$, the total diffusion (DTVO) as well as its axial (DTVO_x) and radial (DTVO_r) components have positive values what corresponds to the loss in the budget of the random temperature variance. It may be also interesting to note that diffusion performed by oscillatory motion is characterised by large amplitudes what seems to be surprising, bearing in mind that diffusion is usually treated as a process typical for random turbulence. The complex character of (DTVO) distributions suggests that term (DTVT) redistributes the random temperature variance along the axial and radial directions of the flow.

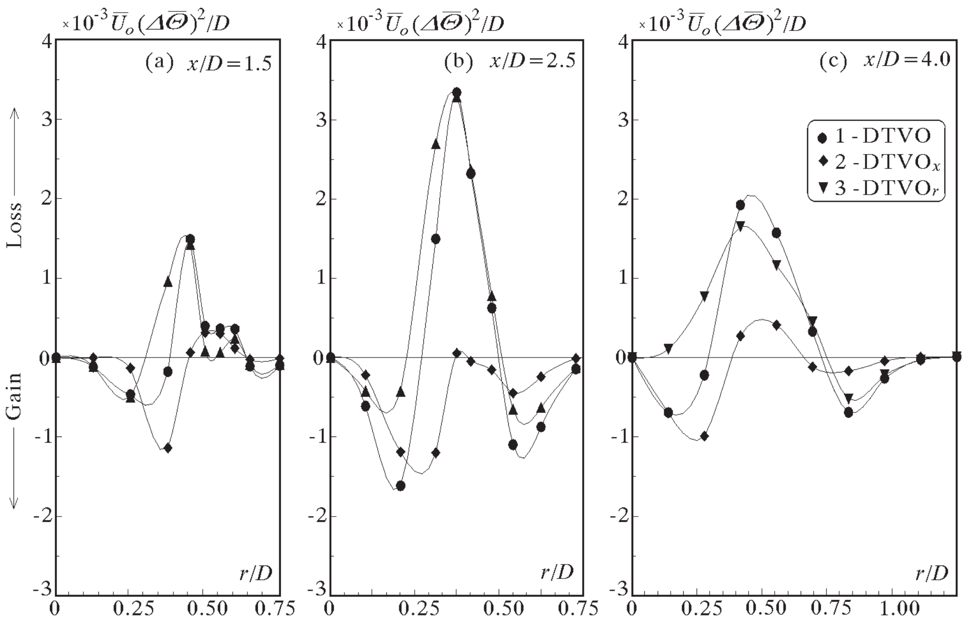

Fig. 8. Radial distributions of axial, radial and total diffusion of random component of temperature variance performed by oscillatory motion at the cross-sections: (a) $x/D = 1.5$, (b) $x/D = 2.5$, (c) $x/D = 4.0$

Production of random temperature variance performed by turbulent heat fluxes (PRHF) was also subdivided into two terms

$$\mathrm{PRHF} = \underbrace{\left(\overline{-u'_x\vartheta'}\right)\frac{\partial\overline{\Theta}}{\partial x}}_{(\mathrm{PRHF}_x)} + \underbrace{\left(\overline{-u'_r\vartheta'}\right)\frac{\partial\overline{\Theta}}{\partial r}}_{(\mathrm{PRHF}_r)}$$

and their distributions have been presented in Fig. 9. Production (PRHF) represents gain in all cross-sections and it is dominated by its radial component (PRHF$_r$). Maxima of (PRHF) and (PRHF$_r$) coincide with the maximum values of mean temperature gradient what is typical for all production terms (El Sayed, 1995). One may expect therefore that term (PRHF) is responsible for generation of random temperature fluctuations characteristic for turbulent mixing processes.

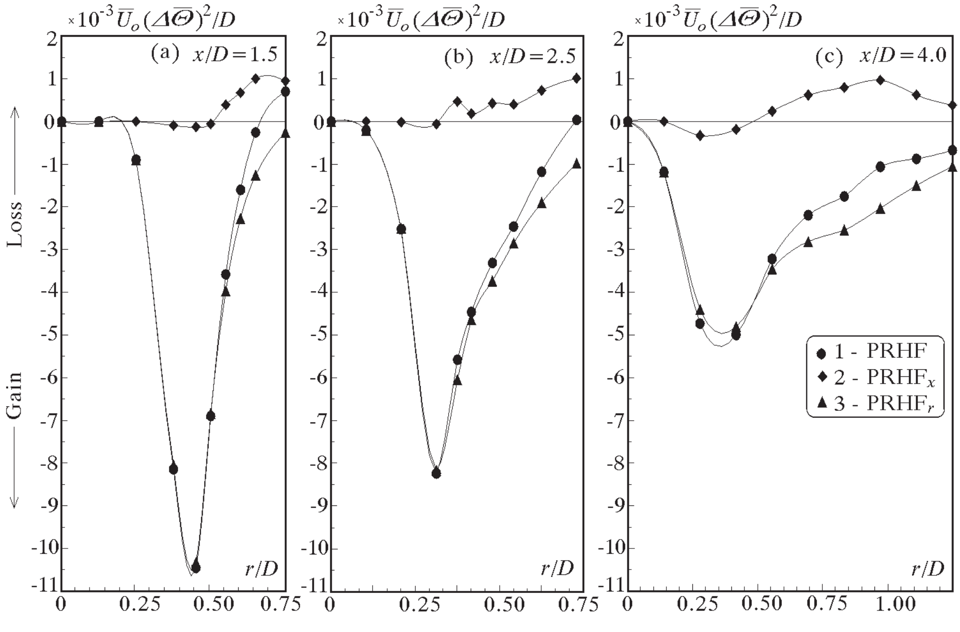

Fig. 9. Radial distributions of axial radial and total production of random component of temperature variance performed by turbulent heat fluxes, at the cross-sections: (a) $x/D = 1.5$, (b) $x/D = 2.5$, (c) $x/D = 4.0$

5. Budget of oscillatory heat fluxes

In order to extend the description of the heat transfer processes performed in the round jet characterized by the presence of coherent structures, the analysis of transport equation for oscillatory heat fluxes has also been performed. Heat fluxes are directional quantities, which explain not only the mechanisms but also they give information about spatial properties of the heat transfer processes. Preliminary analysis performed in (Reynolds and Hussain, 1972) revealed that the amplitudes of circumferential heat fluxes were at least by one order of magnitude smaller than the amplitudes of axial and radial fluxes. That is why the present analysis has been confined to the transport equation of axial and random components of oscillatory heat flux.

The equation of oscillatory heat flux transported in axial direction is written as follows

$$
\begin{aligned}
&\underbrace{\overline{U_x}\frac{\partial}{\partial x}\Big(\overline{\widetilde{u}_x\widetilde{\vartheta}}\Big)+\overline{U_r}\frac{\partial}{\partial r}\Big(\overline{\widetilde{u}_x\widetilde{\vartheta}}\Big)}_{(1)}+\underbrace{\frac{1}{\rho}\overline{\widetilde{\vartheta}\frac{\partial\widetilde{p}}{\partial x}}}_{(2)}- \\
&-\underbrace{\Big(\overline{-\widetilde{u}_x\widetilde{\vartheta}}\Big)\frac{\partial\overline{U_x}}{\partial x}-\Big(\overline{-\widetilde{u}_r\widetilde{\vartheta}}\Big)\frac{\partial\overline{U_x}}{\partial r}}_{(3)}-\underbrace{\Big(\overline{-\widetilde{u}_x\widetilde{u}_x}\Big)\frac{\partial\overline{\Theta}}{\partial x}-\Big(\overline{-\widetilde{u}_x\widetilde{u}_r}\Big)\frac{\partial\overline{\Theta}}{\partial r}}_{(4)}+ \\
&+\underbrace{\overline{(-\langle u_x'\vartheta'\rangle)\frac{\partial\widetilde{u}_x}{\partial x}}+\overline{(-\langle u_r'\vartheta'\rangle)\frac{\partial\widetilde{u}_x}{\partial r}}}_{(5)}+\underbrace{\overline{(-\langle u_x'u_x'\rangle)\frac{\partial\widetilde{\vartheta}}{\partial x}}+\overline{(-\langle u_x'u_r'\rangle)\frac{\partial\widetilde{\vartheta}}{\partial r}}}_{(6)}+ \qquad (5.1) \\
&+\underbrace{\frac{\partial}{\partial x}\Big(\overline{\widetilde{u}_x\widetilde{u}_x\widetilde{\vartheta}}+\overline{\widetilde{u}_x\langle u_x'\vartheta'\rangle}+\overline{\widetilde{\vartheta}\langle u_x'u_x'\rangle}\Big)+\frac{\partial}{r\partial r}\Big[r\Big(\overline{\widetilde{u}_x\widetilde{u}_r\widetilde{\vartheta}}+\overline{\widetilde{u}_x\langle u_r'\vartheta'\rangle}+\overline{\widetilde{\vartheta}\langle u_r'u_x'\rangle}\Big)\Big]}_{(7)}- \\
&-\underbrace{\overline{\nu\widetilde{\vartheta}\Big(\frac{\partial^2\widetilde{u}_x}{\partial x^2}+\frac{\partial^2\widetilde{u}_x}{\partial r^2}+\frac{1}{r}\frac{\partial\widetilde{u}_x}{\partial r}\Big)}}_{(8)}-\underbrace{\overline{a\widetilde{u}_x\Big(\frac{\partial^2\widetilde{\vartheta}}{\partial x^2}+\frac{\partial^2\widetilde{\vartheta}}{\partial r^2}+\frac{1}{r}\frac{\partial\widetilde{\vartheta}}{\partial r}\Big)}}_{(9)}=0
\end{aligned}
$$

where

(1) – Convection of Oscillatory Heat Fluxes (COHFX)

(2) – Redistribution of Oscillatory Heat Fluxes resulting from interaction between the oscillatory temperature T and velocity U and pressure P fields (ROHFTVPX)

(3) – Production of Oscillatory heat fluxes realised by longitudinal component of mean velocity component (POHFVX)

(4) – Production of Oscillatory heat fluxes performed by mean temperature component (POHFTX)

(5) – Production of Oscillatory Heat Fluxes performed by longitudinal, oscillatory velocity component (POHFuX)

(6) – Production of Oscillatory Heat Fluxes performed by oscillatory temperature component (POHFtX)

(7) – Redistribution of Oscillatory Heat Fluxes performed by triple velocity – temperature correlations (ROHFutX)

(8) – Molecular Transport of oscillatory heat fluxes performed by Viscosity (MTVX)
(9) – Molecular Transport of oscillatory heat fluxes performed by Thermal Conductivity of the fluid (MTTVX).

Transport equation of the radial component of heat flux was written in the following form

$$
\begin{aligned}
&\underbrace{\overline{U_x}\frac{\partial}{\partial x}\Big(\overline{\widetilde{u}_r\widetilde{\vartheta}}\Big)+\overline{U_r}\frac{\partial}{\partial r}\Big(\overline{\widetilde{u}_r\widetilde{\vartheta}}\Big)}_{(1)}+\underbrace{\frac{1}{\rho}\overline{\widetilde{\vartheta}\frac{\partial\widetilde{p}}{\partial r}}}_{(2)}-\underbrace{\Big(\overline{-\widetilde{u}_x\widetilde{\vartheta}}\Big)\frac{\partial\overline{U_r}}{\partial x}-\Big(\overline{-\widetilde{u}_r\widetilde{\vartheta}}\Big)\frac{\partial\overline{U_r}}{\partial r}}_{(3)}-\\
&-\underbrace{\Big(\overline{-\widetilde{u}_x\widetilde{u}_r}\Big)\frac{\partial\overline{\Theta}}{\partial x}-\Big(\overline{-\widetilde{u}_r\widetilde{u}_r}\Big)\frac{\partial\overline{\Theta}}{\partial r}}_{(4)}+\underbrace{\overline{(-\langle u'_x\vartheta'\rangle)\frac{\partial\widetilde{u}_r}{\partial x}}+\overline{(-\langle u'_r\vartheta'\rangle)\frac{\partial\widetilde{u}_r}{\partial r}}}_{(5)}+\\
&+\underbrace{\overline{(-\langle u'_x u'_r\rangle)\frac{\partial\widetilde{\vartheta}}{\partial x}}+\overline{(-\langle u'_r u'_r\rangle)\frac{\partial\widetilde{\vartheta}}{\partial r}}}_{(6)}+\underbrace{\frac{\partial}{\partial x}\Big(\overline{\widetilde{u}_x\widetilde{u}_r\widetilde{\vartheta}}+\overline{\widetilde{u}_r\langle u'_x\vartheta'\rangle}+\overline{\widetilde{\vartheta}\langle u'_x u'_r\rangle}\Big)+}_{(7)} \qquad (5.2)\\
&\underbrace{+\frac{\partial}{r\partial r}\Big[r\Big(\overline{\widetilde{u}_r\widetilde{u}_r\widetilde{\vartheta}}+\overline{\widetilde{u}_r\langle u'_r\vartheta'\rangle}+\overline{\widetilde{\vartheta}\langle u'_r u'_r\rangle}\Big)\Big]-\frac{1}{r}\Big(\overline{\widetilde{u}_\varphi\widetilde{u}_\varphi\widetilde{\vartheta}}+\overline{\widetilde{\vartheta}\langle u'_\varphi u'_\varphi\rangle}+2\overline{U_\varphi}\overline{\widetilde{u}_\varphi\widetilde{\vartheta}}\Big)}_{(7)}-\\
&-\underbrace{\overline{\nu\widetilde{\vartheta}\Big(\frac{\partial^2\widetilde{u}_r}{\partial x^2}+\frac{\partial^2\widetilde{u}_r}{\partial r^2}+\frac{1}{r}\frac{\partial\widetilde{u}_r}{\partial r}\Big)-\frac{1}{r}\Big(\frac{2}{r}\frac{\partial\widetilde{u}_\varphi}{\partial r}+\frac{\widetilde{u}_r}{r}\Big)}}_{(8)}-\\
&-\underbrace{\overline{a\widetilde{u}_r\Big(\frac{\partial^2\widetilde{\vartheta}}{\partial x^2}+\frac{\partial^2\widetilde{\vartheta}}{\partial r^2}+\frac{1}{r}\frac{\partial\widetilde{\vartheta}}{\partial r}\Big)}}_{(9)}=0
\end{aligned}
$$

where particular terms have been denoted as:
(1) – Convection of Oscillatory Heat Fluxes (COHFR)
(2) – Redistribution of Oscillatory Heat Fluxes resulting from interaction between the oscillatory temperature T and velocity U and pressure P fields (ROHFTVPR)
(3) – Production of Oscillatory heat fluxes realised by longitudinal component of mean velocity component (POHFVR)
(4) – Production of Oscillatory heat fluxes performed by mean temperature component (POHFTR)
(5) – Production of Oscillatory Heat Fluxes performed by longitudinal, oscillatory velocity component (POHFuR)

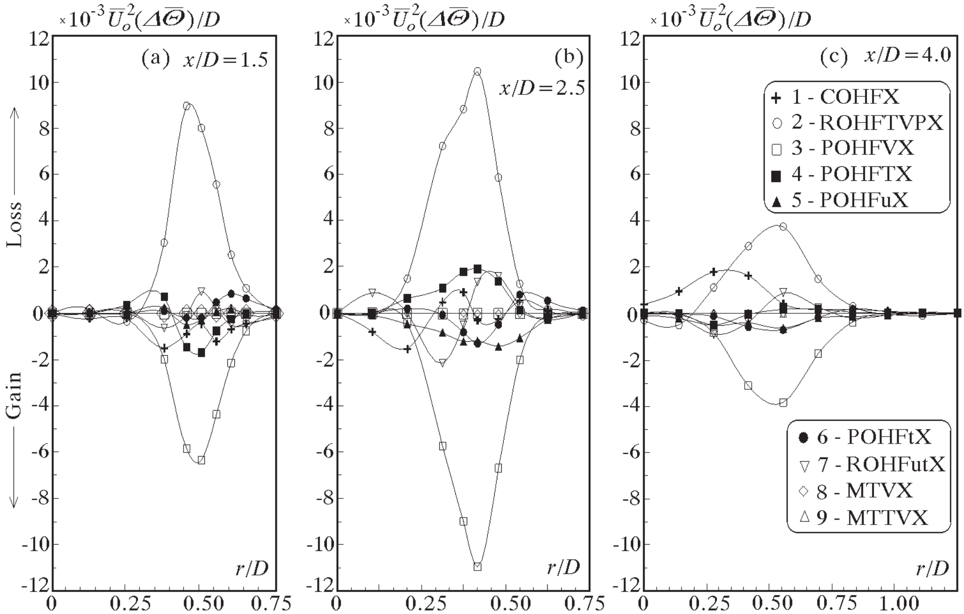

Fig. 10. Budget of oscillatory heat fluxes of longitudinal component, at the cross-sections: (a) $x/D = 1.5$, (b) $x/D = 2.5$, (c) $x/D = 4.0$

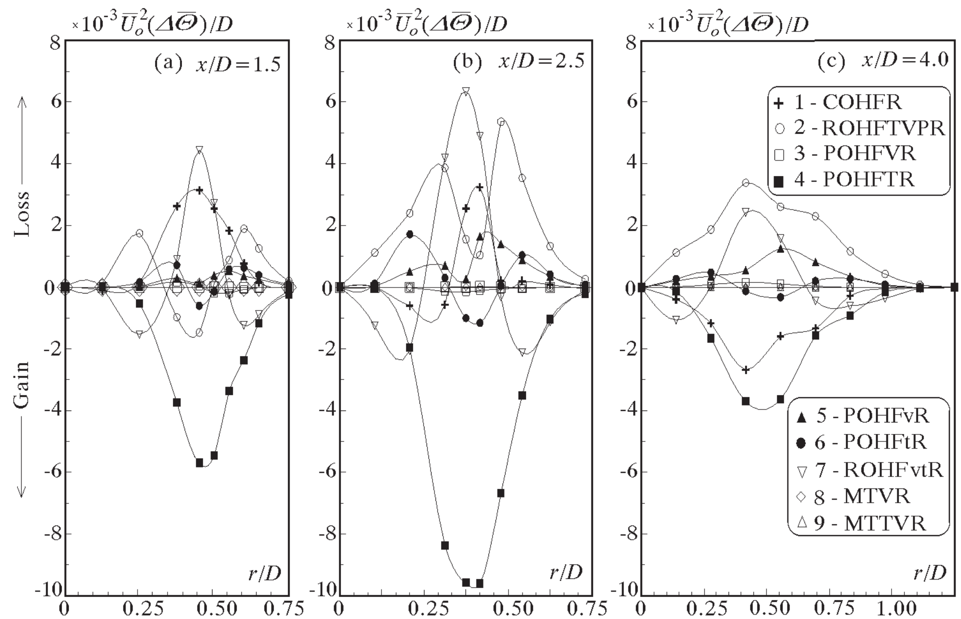

Fig. 11. Budget of oscillatory heat fluxes of radial component, at the cross-section: (a) $x/D = 1.5$, (b) $x/D = 2.5$, (c) $x/D = 4.0$

(6) – Production of Oscillatory Heat Fluxes performed by oscillatory temperature component (POHFtR)
(7) – Redistribution of Oscillatory Heat Fluxes performed by triple velocity – temperature correlations (ROHFutR)
(8) – Molecular Transport of oscillatory heat fluxes performed by Viscosity (MTVR)
(9) – Molecular Transport of oscillatory heat fluxes performed by Thermal Conductivity of the fluid (MTTVR).

The instantaneous temperature and velocity time series allowed to calculate the values of all the terms of Eqs (5.1) and (5.2) except term 2 of both the above equations, which was treated as a closing quantity. Fig. 10 and Fig. 11 present the oscillatory heat flux budgets for axial and radial components which were calculated in three consecutive cross-sections $x/D = 1.5$, 2.5 and 4.0. Budget of the heat flux transported in the longitudinal direction (see Fig. 10) is dominated by convection (COHFX) and production performed by mean velocity (POHFVX). One may also note that transport of radial component of the oscillatory heat flux (see Fig. 11) is under the prevailing influence of convection (COHFR) and production performed by temperature (POHFTR) and this observation is valid in all cross-sections. Following the analyses performed in previous sections, the convections terms of Eqs (5.1) and (5.2) have been decomposed into the axial and the radial directions according to the formulae:

— for axial heat flux component

$$\mathrm{COHFX} = \underbrace{\overline{U_x}\frac{\partial}{\partial x}\left(\overline{\widetilde{u}_x\widetilde{\vartheta}}\right)}_{(\mathrm{COHFX}_x)} + \underbrace{\overline{U_r}\frac{\partial}{\partial r}\left(\overline{\widetilde{u}_x\widetilde{\vartheta}}\right)}_{(\mathrm{COHFX}_r)}$$

— for radial heat flux component

$$\mathrm{COHFR} = \underbrace{\overline{U_x}\frac{\partial}{\partial x}\left(\overline{\widetilde{u}_r\widetilde{\vartheta}}\right)}_{(\mathrm{COHFR}_x)} + \underbrace{\overline{U_r}\frac{\partial}{\partial r}\left(\overline{\widetilde{u}_r\widetilde{\vartheta}}\right)}_{(\mathrm{COHFR}_r)}$$

Distributions of the above terms have been calculated and presented in Fig. 13 and Fig. 14 where one may note that in all cases, the analysed convection is dominated by terms corresponding to the axial direction. This observation agrees well with the results of previous analyses performed for the temperature variance and it may be treated as a typical property of all the convection processes. When looking for characteristic features of both the convection processes, one may note that in the first cross-section $x/D = 1.5$ the

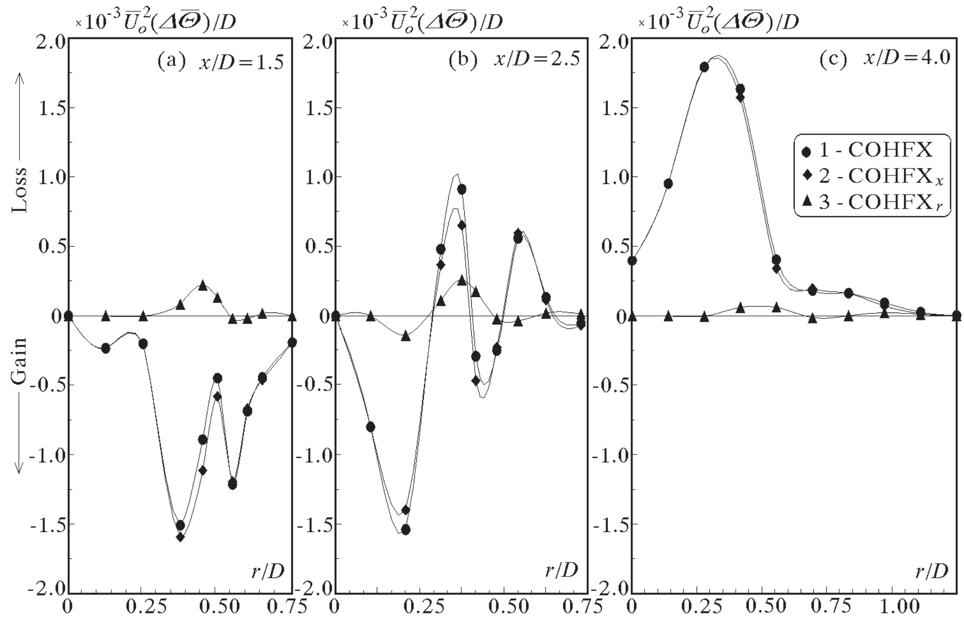

Fig. 12. Radial distributions of axial, radial and total advection of axial oscillatory heat fluxes at the cross- sections: (a) $x/D = 1.5$, (b) $x/D = 2.5$, (c) $x/D = 4.0$

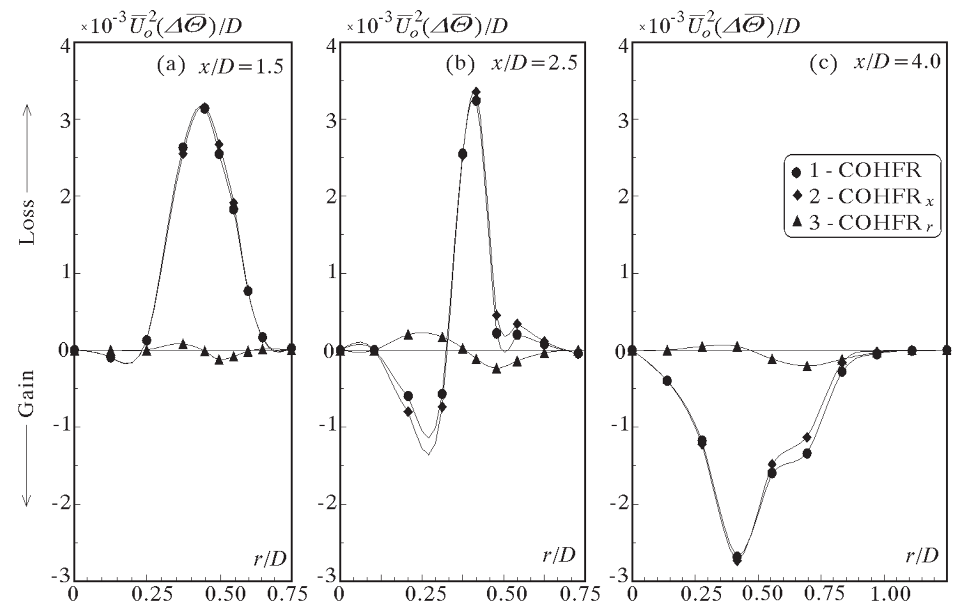

Fig. 13. Radial distributions of axial, radial and total advection of radial oscillatory heat fluxes at the cross- sections: (a) $x/D = 1.5$, (b) $x/D = 2.5$, (c) $x/D = 4.0$

total and axial convection terms have the same sign corresponding to a gain in case of $\overline{\widetilde{u}_x\widetilde{\vartheta}}$ flux and to a loss observed for $\overline{\widetilde{u}_r\widetilde{\vartheta}}$. In the last cross-section analysed (see Fig. 12c and Fig. 13c) one notices the same character but the opposite contributions of axial and radial components of the oscillatory heat flux.

In the cross-section $x/D = 2.5$ where the coherent vortices achieve a maximum coherence (El Sayed, 1995), both convection terms presented in Fig. 12b and Fig. 13b oscillate between loss and gain. It may also be interesting to note that maximum amplitudes of both the convection terms change significantly along the jet axis while at the same time, the maximum amplitude of (COHFR) term is on the average two times larger than the one revealed by (COHFX) term. The next interesting observation concerns the role of viscosity in diminishing the spatial coherence of vortex structures. This phenomenon is seen most clearly in cross-section $x/D = 4.0$ where the convection terms become evidently distorted. The inner jet region $r/D < 0.5$ is characterised by the considerable amplitude of convection terms while in the outer region $r/D > 0.5$ this amplitude tends to zero. It may be expected that viscous shear forces destroy the spatial coherence of the vortex in the outer jet region and result in the decrease of convection of oscillatory heat fluxes. It should however be noted that this tendency is more clearly visible in the case of the (COHFX) term because the radial extent of (COHFR) distribution is larger in the outer jet region (see Fig. 12 and Fig. 13 for comparison). The next important process is the transport of oscillatory heat fluxes in the production, which has been the decomposed as follows:

— for longitudinal heat fluxes

$$\mathrm{POHFVX} = \underbrace{\Big(\overline{-\widetilde{u}_x\widetilde{\vartheta}}\Big)\frac{\partial\overline{U_x}}{\partial x}}_{(\mathrm{POHFVX}_x)} + \underbrace{\Big(\overline{-\widetilde{u}_r\widetilde{\vartheta}}\Big)\frac{\partial\overline{U_x}}{\partial r}}_{(\mathrm{POHFVX}_r)}$$

— for radial heat fluxes

$$\mathrm{POHFTR} = \underbrace{\Big(-\overline{\widetilde{u}_x\widetilde{u}_r}\Big)\frac{\partial\overline{\Theta}}{\partial x}}_{(\mathrm{POHFTR}_x)} + \underbrace{\Big(-\overline{\widetilde{u}_r\widetilde{u}_r}\Big)\frac{\partial\overline{\Theta}}{\partial r}}_{(\mathrm{POHFTR}_r)}$$

As can be seen in Fig. 14 and Fig. 15, both these terms reveal a very similar behaviour in all consecutive cross-sections. In particular, their maximum amplitude occurs in $x/D = 2.5$ cross-section what means that both these processes are closely correlated with the spatial coherence of organised vortices. Both these distributions are dominated by longitudinal components what

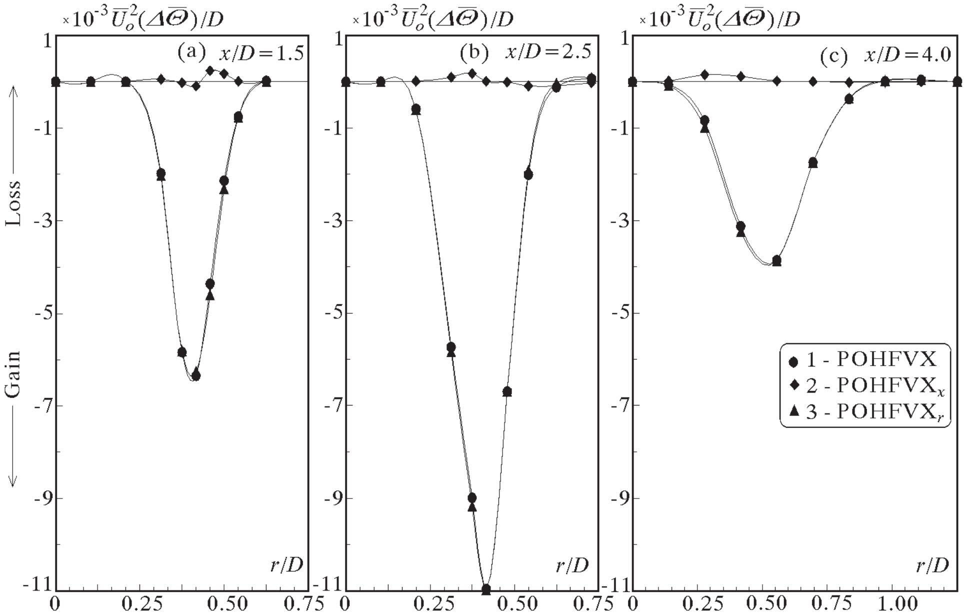

Fig. 14. Radial distributions of axial, radial and total production of axial, oscillatory heat fluxes realised by longitudinal component of mean velocity component, at the cross-sections: (a) $x/D = 1.5$, (b) $x/D = 2.5$, (c) $x/D = 4.0$

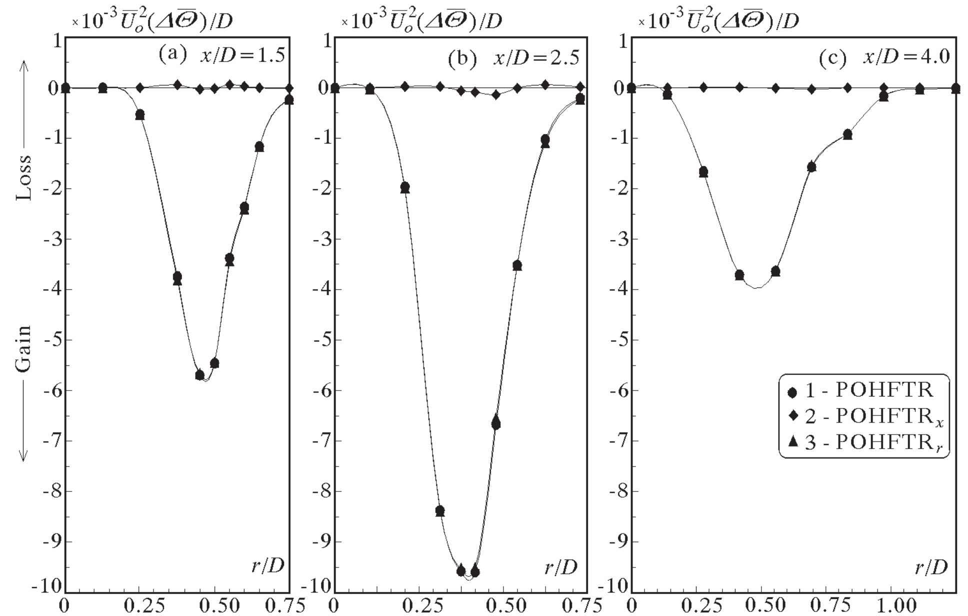

Fig. 15. Radial distributions of axial, radial and total production of radial, oscillatory heat fluxes performed by mean temperature component at the cross-sections: (a) $x/D = 1.5$, (b) $x/D = 2.5$, (c) $x/D = 4.0$

results from the obvious relations

$$\frac{\partial \overline{U_x}}{\partial r} \gg \frac{\partial \overline{U_x}}{\partial x} \qquad\qquad \frac{\partial \overline{\Theta}}{\partial r} \gg \frac{\partial \overline{\Theta}}{\partial x}$$

One may also note that both these distributions become nonsymmetric due to the action of shear forces what is most clearly visible in the outer jet region at $x/D = 4.0$ cross-section (see Fig. 14 and Fig. 15).

6. Conclusions

Within the research presented here, an analysis of temperature variance and oscillatory heat fluxes has been presented. The computed distributions of particular terms allowed to obtain a quantitative information about the intensity of heat transfer processes.

Experimental limitations did not allow to calculate all the quantities appearing in the transport equations and that is why some terms had to be treated as closing quantities. One should note however that relatively smooth distributions of the closing terms in all budgets suggest a good accuracy of the analyses.

The results of the research performed allowed to formulate a considerable amount of observations but their number is certainly too large to be discussed here. However, one may state that the transport processes of temperature variance and oscillatory heat fluxes are under a distinct influence of coherent structures.

Acknowledgements

The work has been funded by the State Committee for Scientific Research (KBN, Warsaw) under the Statutory Funds BS – 03 301/98.

References

1. Drobniak S., 1986, *Coherent Structures of Free Axisymmetric Jet*, Monograph Series No. 1, Technical University of Częstochowa
2. Drobniak S., Elsner J.W., 1986, Coherent Structures and their Relation to Instability Processes in a Round, Free Jet, In: *Advances in Turbulence*, Springer-Verlag, Berlin

3. Drobniak, S., Elsner J.W., El Sayed Abou El Kassem, 1997, The Internal Structure of the Column-Mode Coherent Vortex in Free Axisymmetric Jet, *Journal of Theoretical and Applied Mechanics*, **35**, 2, 347-368

4. Drobniak S., Elsner J.W., El Sayed Abou El Kassem, 1998, The Relationship Between Coherent Structures and Heat Transfer Processes in the Initial Region a Round Jet, *Experiments in Fluids*, **24**, 225-237

5. El Sayed Abou El Kassem, 1995, An Analysis of Heat Transfer Processes in the Coherence Region of a Round Free Jet, Ph.D. Thesis, Technical University of Częstochowa

6. El Sayed Abou El Kassem, Drobniak S., Elsner J.W., 1998, Experimental Analysis of Internal Energy Transport in the Presence of Coherent Motion, *International Journal of Heat and Mass Transfer*, **41**, 3, 635-643

7. Elsner J.W., Drobniak S., 1994, Transport Processes Realized by Organized Vortex Structures, *Proc. XI National Conference on Fluid Mechanics*, **2**, 19-24

8. Elsner J.W., Klajny R., Drobniak S., 1992, Contribution of Coherent Structures to Heat and Mass Transport in the Round, Free Jet, *Proc. VIII Symposium of Heat and Mass Transfer*, 149-156

9. Favre-Marinet M., 1986, Structure Coherentes Dans un Jet Ronde Excite, These Doct. Sc., USTMG et INPG, Grenoble

10. Favre-Marinet M., 1989, Coherent Structures in a Round Jet, *Proc. of the von Kármán Institute for Fluid Dynamics, Lecture Series*, **3**

11. Pełka P., 1999, An Analysis of Coherent Structures Influence on the Temperature Field in a Free Round Jet, Ph.D.Thesis, Technical University of Czestochowa

12. Reynolds W.C., Hussain A.K.M.F., 1972, The Mechanics of Organized Wave in Turbulent Shear Flow. Part 3, *J. Fluid Mech.*, **54**, 263-288

13. Wygnanski I.I., Peterson R.A., 1987, Coherent Motion in Excited Free Shear Flows, *AIAA Journal*, **25**, 2, 211-213

Struktury koherentne i transport wariancji temperatury oraz oscylacyjnych strumieni ciepła w strudze kołowej

Streszczenie

W pracy przedstawiono wyniki eksperymentalnej analizy procesów transportu ciepła zachodzących w początkowym obszarze osiowosymetrycznej strugi swobodnej w obecności struktur koherentnych stymulowanych polem akustycznym. Przyjęto, że

parametrami, przy pomocy których można w sposób jakościowy i ilościowy opisać zachodzące w przepływie procesy są wariancja temperatury i oscylacyjne strumienie ciepła. Wariancja temperatury może być bowiem traktowana jako miara intensywności transportu ciepła, podczas gdy strumienie ciepła opisują jego przemieszczanie się w obszarze przepływu. Uzyskane na drodze eksperymentalnej przestrzenne rozkłady obu wielkości fizycznych, uzupełnione fizykalną analizą ich równań transportu, pozwoliły na rozpoznanie procesów przemieszczania się ciepła w przepływie w obecności struktur koherentnych.

Manuscript received February 6, 2001; accepted for print April 16, 2001